A major purpose of the Technical Information Center is to provide the broadest dissemination possible of information contained in DOE's Research and Development Reports to business, industry, the academic community, and federal, state and local governments.

Although a small portion of this report is not reproducible, it is being made available to expedite the availability of information on the research discussed herein.

LA-UR -86-1299
CONF-860551--2

RECEIVED BY OSTI MAY 1 2 1986

LA-UR--86-1299

DE86 010185

TITLE: COMPACT REVERSED-FIELD PINCH REACTORS (CRFPR)

AUTHOR(S): R. A. Krakowski, R. L. Miller, C. G. Bathke, R. L. Hagenson (Phillips Petroleum Company Bartlesville, OK), C. Copenhaver, and K. A. Werley

SUBMITTED TO IAEA Technical Committee and Workshop on Fusion Reactor Design and Technology
Yalta, USSR
May 26 - June 6, 1986

COMPACT REVERSED-FIELD PINCH REACTORS (CRFPR)*

R. A. Krakowski, R. L. Miller, C. G. Bathke,
R. L. Hagenson,** C. Copenhaver, K. A. Werley
Los Alamos National Laboratory, Los Alamos, NM 87545 USA

ABSTRACT
The unique confinement properties of the Reversed-Field Pinch (RFP) are exploited to examine physics and technical issues related to a compact, high-power-density fusion reactor. This resistive-coil, steady-state, toroidal device would use a dual-media power cycle driven by a fusion power core (FPC, i.e., plasma chamber, first wall, blanket, shield, and coils) with a power density and mass approaching values characteristic of pressurized-water fission reactors. A 1000-MWe(net) base case is selected from a comprehensive trade-off study to examine technological issues related to operating a high-power-density FPC. After describing the main physics and technology issues for this base-case reactor, directions for future study are suggested.

1. INTRODUCTION

The reversed-field pinch (RFP)[1-3] is a toroidal axisymmetric magnetic configuration in which the plasma is confined by a combination of a poloidal field, B_θ, generated by a current flowing in the plasma, and a toroidal field, B_ϕ, produced partly by currents flowing in the plasma and partly by external coils. The RFP, along with the tokamak and the spheromak, belongs to the toroidal pinch family of confinement systems. The distinguishing feature of the RFP, as is shown in Fig. 1, is that a) $B_\theta \simeq |B_\phi|$ within the plasma and b) the toroidal field is reversed in the outer region with respect to the value on the axis. The safety factor, $q = r_p B_\phi / R_T B_\theta$, where the minor and major radii of the plasma are r_p and R_T, respectively, can be made less than unity, giving large plasma currents, strong ohmic heating, low magnetic fields at coils, and a close coupling of poloidal and toroidal circuits through the plasma and leading to new options for current drive/sustainment. The fundamental property of the RFP (and spheromak) is that the field configuration is a near-minimum-energy state[4,5] to which the plasma relaxes; the generation of the reversed field is a natural consequence of this relaxation process.

The RFP physics characteristics[3] lead to a poloidal-field-dominated plasma and the promise for improved commercial reactors. Early RFP reactor studies were based on superconducting magnets.[6] This approach led to the features of low power density (~ 0.5 MWt/m^3 or ~ 50 kWe/tonne, based on the fusion power core) similar to that proposed for tokamaks,[7] stellarators,[8-9] mirrors,[10] and other alternative fusion concepts.[11] These low-power-density systems would be costly because of the inefficient use of the fusion power core.[12,13] The compact RFP reactor (CRFPR) was suggested[14-16] as a means to increase the fusion-power-core power density to values which are comparable to

*This work performed under the auspices of USDOE/Office of Fusion Energy.
**Phillips Petroleum Company, Bartlesville, OK 74004 USA

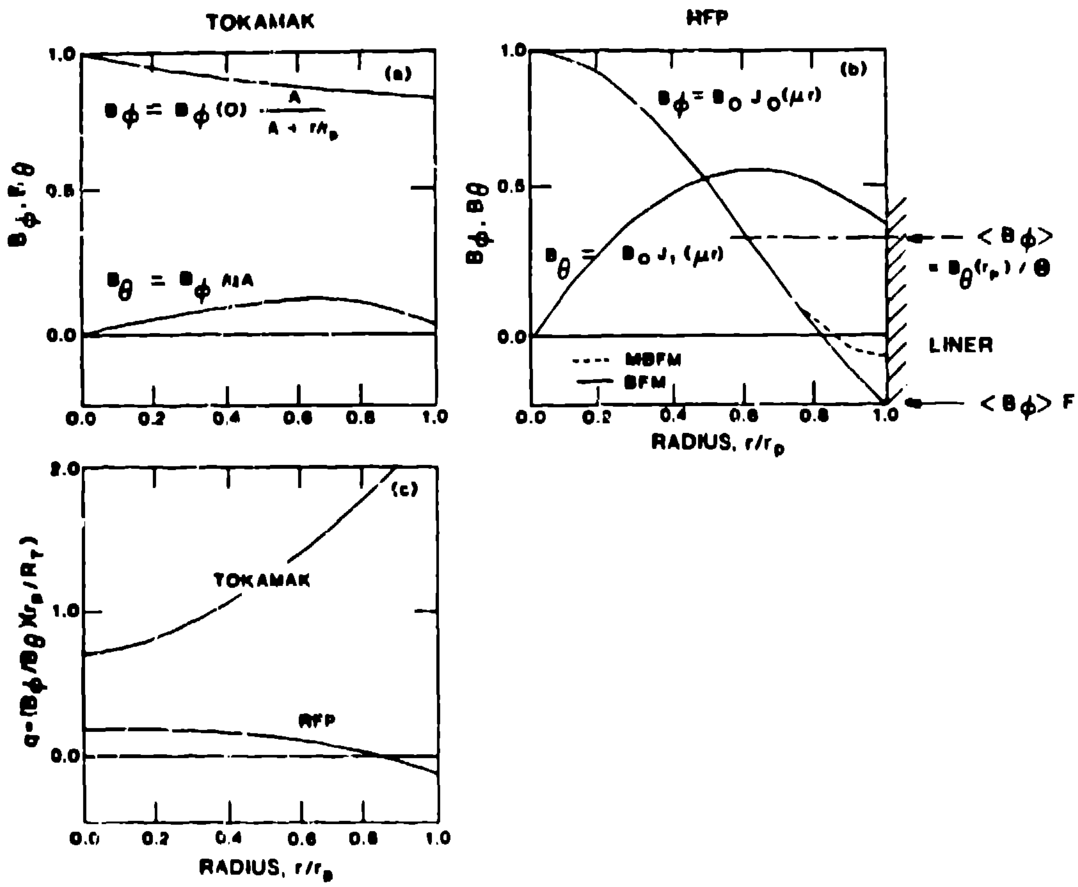

Fig. 1. Comparison of tokamak(a) and RFP(b) field profiles across the plasma minor cross section together with the radial variation of the safety factor q for both systems(c). The profiles shown are based on analytic models of the field distributions, which are a reasonable approximation to experiment.[3]

fission power systems (15 MWt/m^3 or 1000 kWe/tonne for a pressurized-water fission reactor), and beyond threshold economic targets (> 100-200 kWe/tonne) suggested[17] for fusion in general.

The general design approach, tradeoffs, and features of the CRFPR design are described in Sec. 2. After summarizing key physics and technology issues for that design in Sec. 3., future directions are described in Sec. 4. A brief conclusion is given in Sec. 5.

2. COMPACT RFP REACTOR DESIGN

The main effort to date has been applied to a 1000-MWe(net) design operated at high neutron wall loading ($I_w \approx 20$ MW/m^2) using pumped-limiter impurity control and oscillating-field current drive (OFCD) to achieve steady-state, high-power-density operation. The design basis, tradeoffs, alternatives, and the basecase are described.

2.1. Design Basis. The RFP physics described in Refs. 1-3 have been combined into a comprehensive systems analysis[14-16] to provide a range of reactor designs optimized for minimum cost of electricity (COE) through a comprehensive search of key plasma and reactor characteristics. For a given net-electric-power output, a range of plasma dimensions were matched with a cost-optimized FPC for a range of plasma parameters (beta, profiles, ignition $n\tau_E$, temperature, etc.) and engineering variables (efficiencies, FPC lifetimes, coil parameters, replacement schedules, unit costs, etc.). This procedure yields a global energy confinement time, τ_E(OPT), required to assure a minimum-cost reactor. The experimental energy confinement time, τ_E(PHYS), can be derived from the ohmic-scaling extrapolations[3,14-16] of the form $\tau_E(\mathrm{PHYS}) = C_\nu I_\phi^\nu r_p^2 f(\beta_\theta)$, where ν and C_ν are fitting constants, $f(\beta_\theta) = (\beta_{\theta c}/\beta_\theta)^P$, and $\beta_{\theta c} = 0.13$ is a critical beta above which τ_E(PHYS) is assumed to diminish according to $f(\beta_\theta)$. The difference between τ_E(OPT) and τ_E(PHYS) gives a margin that measures the difference between the reactor goal, the physics extrapolation, and the ability to achieve a minimum-COE system.

Typical optimized COEs are plotted on Fig. 2, which shows the minimum-COEs are design point as well as sensitivites to confinement scaling (constant-ν curves), net electric power (constant-P_E curves), and neutron first-wall loading (constant-I_w curves). The P_E, ν, and I_w grid given on Fig. 2 illustrate the trade-off between physics (ν, r_p), economic (COE, P_E), and technology (I_w, r_p) requirements. Two 1000-MWe design points have been selected from the ensemble of minimum-COE designs and are summarized on Table I; the fully minimum-COE design at I_w = 20 MW/m² is termed CRFPR(20), and a somewhat more costly I_w = 5-MW/m² design is termed CRFPR(5). Most of the conceptual engineering design effort to date has been performed for the CRFPR(20) design.[14,15] Although the dependence of COE on FPC size and neutron wall loading is weak, the 20-MW/m², minimum-COE design was selected in order to examine technological limits required to assure a single-piece FPC maintenance scheme [~ 800-tonne poloidal-field coils (PFC), ~ 300-tonne reactor torus]. Upon computing the equilibrium from the coil set suggested by the systems code, adjusting the blanket and shield thickness to accommodate the neutronics analysis of a thin $Pb_{83}Li_{17}$-cooled blanket and a water-cooled first-wall, limiter, and shield, and performing a detailed plasma/circuit simulation, the reactor cross section and FPC design shown in Fig. 3 emerged.[16] This design was subject to engineering analysis to determine more precise reactor parameters. General engineering features of the CRFPR(20) design are summarized in Table II, and Fig. 4 gives a comparison of FPC size for I_w = 5, 10, and 20-MW/m² designs selected from the 1000-MWe(net) minimum-COE curve on Fig. 2.

2.2. Description of FPC. An FPC integration study was performed [14,15] to translate the parameters suggested in Table II into a conceptual engineering design. The following set of engineering constraints was applied:

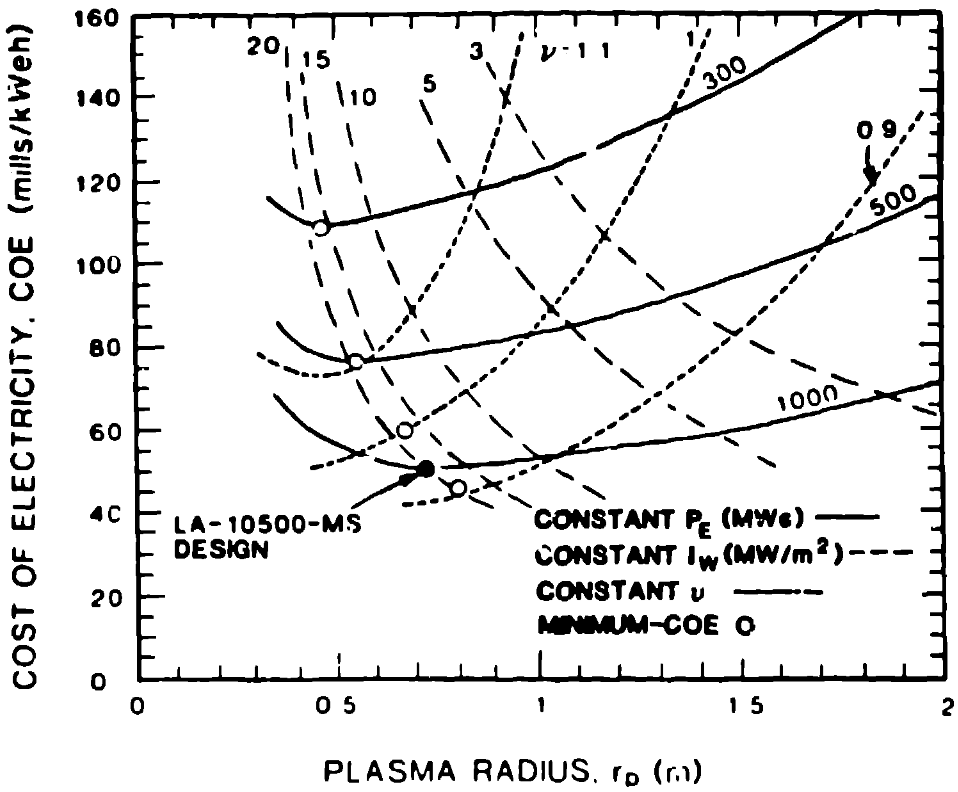

Fig. 2. Dependence of COE ("then-current" 1980 dollars) on plasma radius, r_p, for a range of net-electric powers, P_E, for $A = R_T/r_p \approx 5.35$. Also shown are lines of constant neutron wall loadings, I_w (MW/m^2). The condition where $\tau_E(OPT) = \tau_E(PHYS)$ is also shown for $\tau_E(PHYS) = C_\nu I_w^\nu r_p^2 f(\beta_\Theta)$ scaling for a range of ν values. The minimum-COE design for a given P_E is indicated by the circles, and the required I_w and ν values are indicated.

i) Primary and secondary stresses less in the water-cooled first wall and limiters less than a fifth of the yield stress.

ii) PbLi blanket pressure below ~ 0.7 M Pa (≲ 100 psi).

iii) Pressurized-water coolant velocity below ~ 10 m/s.

iv) Maximum copper-alloy high-heat-flux temperature below ~ 400°C.

v) Maximum structural (HT-9 ferritic alloy) temperature in contact with PbLi below ~ 500°C.

vi) Critical-heat-flux limits for pressurized-water coolant specify a ≳ 10-K subcooling at typical PWR coolant conditions (15.6 MPa or 2,200 psi, 330°C boiling point).

TABLE I

SAMPLE COMPACT RFP REACTOR DESIGN POINTS
FOR THE MINIMUM-COE 1000-MWe(net) CASE AND
A CASE OF LOWER FUSION NEUTRON FIRST-WALL LOADING

DEVICE	CRFPR(20)[a]	CRFPR(5)
Neutron first-wall loading, I_w(MW/m²)	19.5	5.0
Net electrical power, P_E(MWe)	1,000.	1,000.
Total thermal power, P_{TH}(MWt)	3,365.	3,609.
Recirculating power fraction, $1/Q_E$	0.185	0.208
Plasma minor radius, r_p(m)	0.71	1.42
Plasma major radius, R_T(m)[b]	3.8	7.6
Plasma volume, V_p(m³)	37.8	302.5
Plasma power density, P_F/V_p(MW/m³)	72.4	9.6
Plasma temperature, T(keV)	10.0	10.0
Plasma density, n(10²⁰/m³)	6.3	2.3
Average beta, β_θ[c]	0.23	0.23
Plasma energy confinement time, τ_E(s)	0.23	0.70
Plasma thermal diffusivity,[d] χ_E(m²/s)	0.41	0.54
Field at plasma, B_θ(T)	5.2	3.0
Peak field at coil, $B_{\theta c}$(T)	4.5	2.6
Plasma current, I_ϕ(MA)	18.4	21.6
Plasma current density, j_ϕ(MA/m²)	11.2	3.41
FPC volume, V_{FPC}[e](m³)	285.	1,042.
FPC mass, M_{FPC}(tonne)	1,105.	2,000.
FPC power density, P_{TH}/V_{FPC}(MWt/m³)	11.8	3.5
FPC mass utilization, M_{FPC}/P_{TH}(tonne/MWt)	0.33	0.55
FPC mass power density, $1000\ P_E/M_{FPC}$(kWe/tonne)	905.0	500.0
FPC cost as fraction of total direct cost[f]	0.045	~0.05
Unit Direct Cost, UDC ($/kWe)[g]	1,007.	1,169.
Cost of Electricity, COE(mills/kWeh)[g]	48.4	55.5

(a) Values reported are derived from a systems code and differ somewhat from final design values derived from conceptual subsystem design and plasma simulations, as reported in Ref. 14 and subsequently modified by the Ref. 15 study.

(b) Plasma aspect ratio preserved at $A = R_T/r_p = 5.35$, which is a minimum-COE value, but this minimum is very shallow. Blanket design adjustments driven by Ref. 15 follow-on study increased A to 5.5.

(c) Includes ~ 0.03 for steady-state alpha-particle pressure, total (volume-average) beta is ~ 0.12.

(d) Taken as ~ $(3/16)r_p^2/\tau_E$ for a parabolic temperature and flat density profile.

(e) Fusion power core, includes plasma chamber, first-wall/limiters, blanket, shield, and coils; excludes coolants.

(f) Compared to 0.255 for STARFIRE[7] and 0.305 for MARS.[10]

(g) 1980 dollars, with COE given as a "then-current" value (i.e., includes both interest and escalation incurred during the construction period) and Ref. 14 cost database used. Reduction by a factor of ~ 1.79 converts these costs to 1980 constant dollars, and an increase by a factor of 1.348 converts these costs to a 1986 basis.

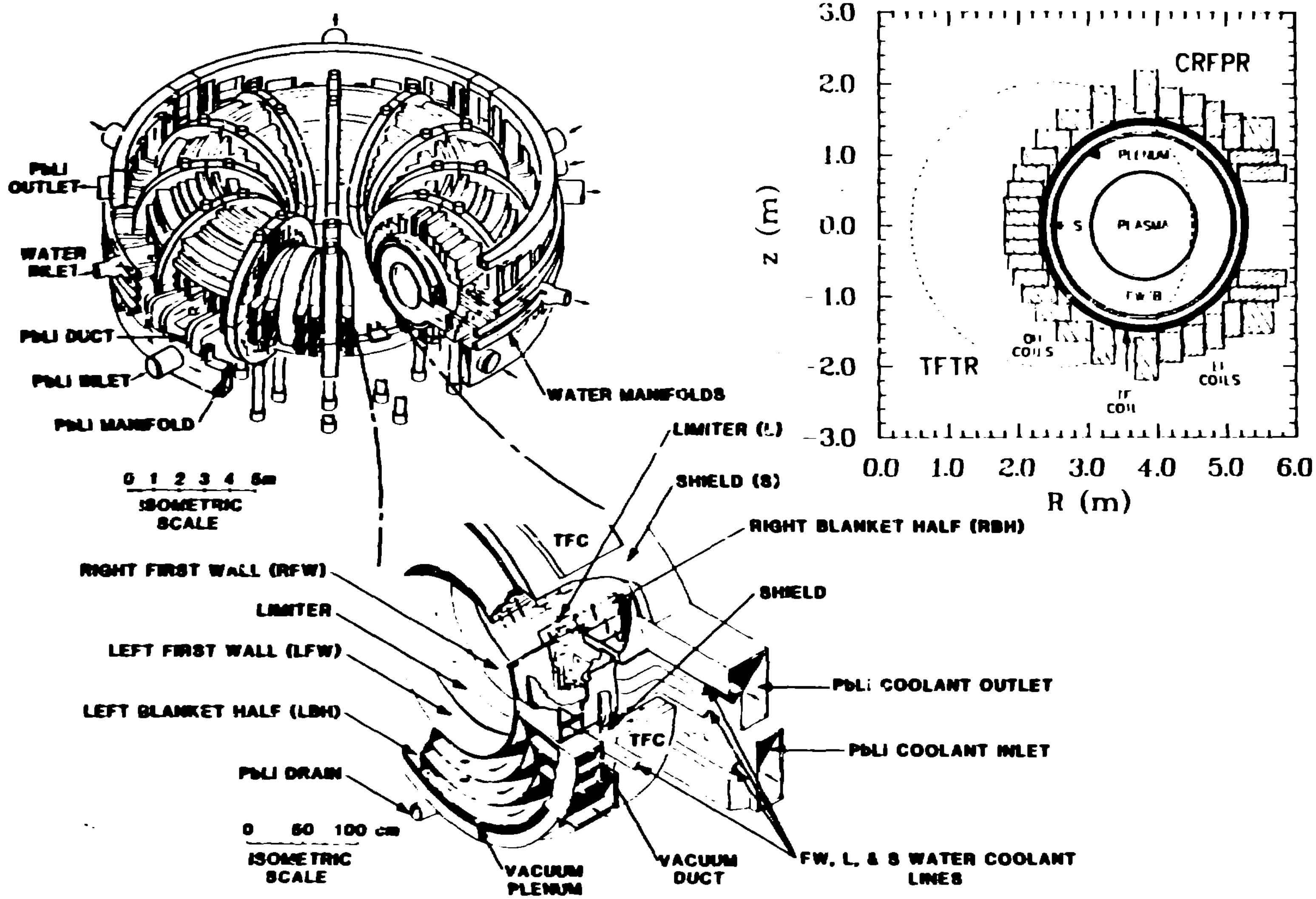

Fig. 3. Isometric view of CRFPR fusion power core based on engineering integration studies reported in Ref. 14 and 15. The reactor torus, defined as the plasma chamber, first wall, limiter, blanket, shield/structure, and TF coils (i.e., the FPC less the ~ 800-tonne PF coils), is installed and replaced as a single ~ 300-tonne unit (drained of PbLi coolant).

TABLE II

KEY CRFPR ENGINEERING PARAMETERS AND CHARACTERISTICS FOR THE CRFPR(20) DESIGN FROM REF. 15[a]

Net/gross electrical power, P_E(MWe)/P_{ET}(MWe)	1000./1256.
Total thermal power, P_{TH}(MWt)	3473.
Gross power-conversion efficiency, η_{TH}	0.369
Recirculation power fraction, ε	0.204
Overall plant availability, p_f	0.76 (15 MWyr/m² life)
Major/minor plasma radius, R_T/r_p(m)	3.9/0.71
Plasma volume, V_p(m³)	38.8
First-wall area, A_{FW}(m²)	115.
Neutron first-wall loading, I_w(MW/m²)	19.0
Number of toroidal sectors, N	24.[a]
Maximum field at magnet, $B_{\theta c}$ (T)	4.5[b]
Field at plasma axis/edge, $B_\phi(0)/B_\theta(r_p)$(T)	9.5/5.2
Average poloidal/total beta, β_θ/β	0.23/0.12
Average density/temperature, n(10²⁰/m³)/T(keV)	6.6/10.0
Plasma burn mode	Continuous/ignited[c]
Plasma heating method (startup)	Ohmic (246 V-s total, 26 V-s, ohmic)
Plasma current/ohmic power (MA/MW)	18.4/25.3
Plasma impurity control	Poloidal pumped limiter (24, 38% first wall)
First-wall/limiter	MZC copper alloy (water-cooled)
Blanket/shield structure	HT-9 steel (water-cooled second wall)
Tritium-breeding medium	PbLi(35 MW/m³ average), TBR = 1.06(2-D)
Primary coolant	PbLi (poloidal flow, 0.6-m-thick)
Shield	Stainless steel (0.1-m-thick, water-cooled)
Thermal-conversion method	Dual-media (46.3% H_2O, 5.37% PbLi) steam
FPC Masses (tonne; 310 m³, 3.58 tonne/m³, 11.2 MWt/m³, 0.32 tonne/MWt)	
• Limiters[e]	8.4
• First wall	1.8
• Second wall[e]	9.9
• Blanket[f]	48.2
• Shield	159.6.6
• TFC (Subtotal)	76.2(304.)
• OHC	400.
• EFC	413.
Total	1117.

(a)For off-site fabrication purposes only, single-piece FPC maintenance is envisaged for this ~ 304-tonne system (first wall, blanket, shield, toroidal-field coils), to which is added a separate 813-tonne poloidal-field coil set and ~ 943 tonne of PbLi coolant. Modest differences between this and Table I reflect adjustments in carrying the systems code design (Table I) into a conceptual engineering design phase.[15]

(c)At the OHC during the burn, 9.2 T during startup. Peak field at the TFC is 0.7 T, with the plasma dynamo providing a major part of the toroidal flux during startup. The TFC/OHC/EFC power consumption is 12.6/73.0/53.5 MWe, with the OHC power going to zero upon initiation of oscillating-field current drive (OFCD).

(d)Based on OFCD at 50 Hz with $\delta\Phi/\Phi$ ~ 0.035 toroidal flux swing, $\delta V_\phi/\langle I_\phi f_\phi R_p\rangle$ = 100, $\delta I_\phi/I_\phi$ ~ 0.01 plasma current swing. These values are preliminary estimates.

(e)Includes manifolds and headers.

(f)Includes inlet/outlet ducts, but not 925-tonne PbLi coolant.

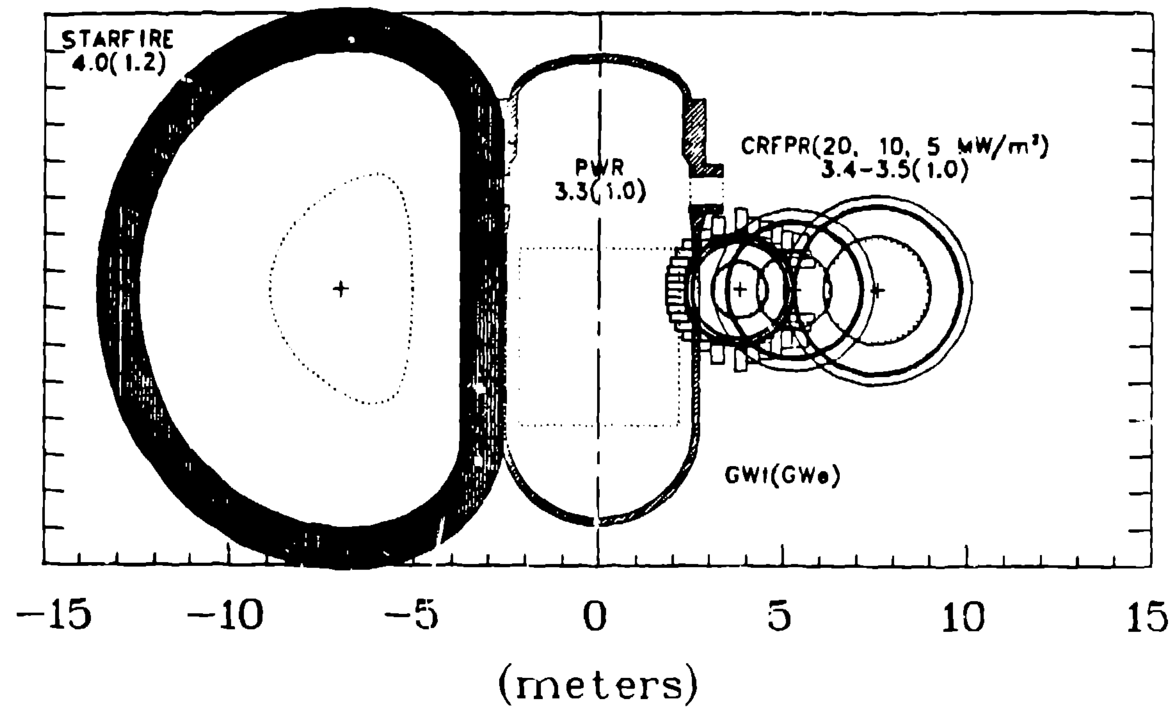

Fig. 4. Comparison of fusion-power-core (FPC) sizes for the CRFPR(5), CRFPR(10), and CRFPR(20) designs with the STARFIRE[7] tokamak and a (British) pressurized-water fission reactor pressure vessel.

vii) Thermal-conversion efficiency taken as $\eta_{TH} = 0.75\eta_{GEN}\eta_I$ ($\eta_{GEN} = 0.98$), where η_I is an ideal conversion efficiency for a dual-media power conversion system.[14,15]

viii) No structural sputtering margin (coatings, tiles, cold/dense radiating plasma edge required).

ix) Self-cooled PbLi blanket MHD pressure modeled in one dimension without recourse to the use of sandwiched electrical insulators.

The basic FPC geometry shown in Fig. 3 is a single-piece reactor torus (i.e., FPC less the PFCs) constructed from 24 sectors that have been joined into a single unit at the 0.1-m-thick, water-cooled, steel structural shield. Flow in the self-cooled PbLi/ferritic-steel (HT-9) blanket is in the direction of the dominant poloidal field. Because of the high heat loads expected for the limiter-based CRFPR(20) design summarized in Table II, a dual-media pressurized-water/flowing-PbLi coolant system was adopted. The limiter, first wall, second wall (i.e., first structure wall of the PbLi blanket), and shield are each cooled by separate, single-pass, pressurized-water circuits that share common input and output headers, but have separate manifolds. The second wall serves as the return leg for the first-wall water coolant. A mechanical separation between the second wall and the containing structure for the PbLi breeder/coolant may be possible, depending on achievable contact thermal resistances.[15,18] Separate cooling of the inside structural wall is necessary for the CRFPR(20) design in order to hold ~ 500°C corrosion related temperature limits imposed at the PbLi/HT-9 interface. The conditions under which separate cooling of the blanket structure by pressurized water can be eliminated requires a neutron first-wall loading below ~ 5 MW/m^2 for systems based on pumped-limiter impurity control[15]; this limit is set largely by the physical heat flux at the first wall and limiter and can be higher for the divertor-based designs presently being examined. Access for all coolant and vacuum lines would be at the outboard equatorial plane (Fig. 3), where both PbLi and pressurized-water coolants are manifolded for power distribution to the respective steam generators.

Starting with the plasma, $P_N = 2186.8$ MW of 14.1-MeV neutron power contributes to volumetric heating in the limiter, first wall, second wall, blanket, shield, and coils. The steady-state plasma must also radiate, conduct, and convect a power equal to the sum of the alpha particles, $P_\alpha = 516.5$ MW, and the ohmic dissipation, $P_\Omega = 25.3$ MW. A fraction of $P_\alpha + P_\Omega$ is radiated uniformly over the first-wall and limiter surfaces, whereas the remaining fraction $1 - f_{RAD}$ is conducted/convected, with the fraction f_L of $(1 - f_{RAD})(P_\alpha + P_\Omega)$ actually reaching the limiter surfaces. The nuclear and direct plasma power reaching the limiter, first wall, second wall, and shield are transported to the thermal conversion cycle by pressurized-water coolant, whereas the nuclear heating in the PbLi-cooled blanket is delivered to the power cycle at a higher temperature. Of the total recoverable thermal power, 1607.5 MWt or 46.3% is delivered through the pressurized-water coolant loop. The energy deposited in the near-room-temperature coils is 212.0 MWt, 66% of which (139.1 MWt) results from ohmic dissipation. Hence, 11% of the gross electric power would be recirculated to supply resistive losses in the TFC and FPC sets, and 2.2% is recirculated directly to the plasma, which, when combined with an added 7% recirculated to auxiliary plant needs, amounts to a total recirculating power fraction of $\varepsilon \simeq 0.20$. The FPC thermalhydraulic design and optimization gives an overall thermal-conversion efficiency of $\eta_{TH} = 0.369$ for this dual-media thermal cycle, which when combined with ε and a generator efficiency of $\eta_{GEN} = 0.98$ gives an overall plant efficiency of $\eta_p = 0.288$.

The FPC size of the CRFPR(20), including the main PbLi manifold, is small (1,117 tonne, 362 m^3) compared to that for the STARFIRE tokamak[7] (~ 23,200 tonne, 8,100 m^3) or MARS tandem-mirror[10] (~ 23,300 tonne, 11,650 m^3) reactors. Several plant layouts were considered in order to quantify the possibility of both vertical- and horizontal-replacement single-piece maintenance schemes[15,16] for the reactor torus. Generally, the ~ 800-tonne PFC set would be moved in quadrants and would be life-of-plant items, whereas the ~ 300-tonne reactor torus contained within the PFC set would be installed and replaced as a single unit once a year. Approximately 10-14 days would be required for a FPC changeout,[15,16] which is within the 28 days allowed for scheduled maintenance (includes 120 days every 10 years for turbine overhaul); combined with 60 days/year for unscheduled maintenance, the plant availability is 76%. The replacement cost for the first wall and blanket amounts to 3.5% of the (constant-dollar) COE.

3. TECHNICAL ISSUES

3.1. Physics and Plasma Engineering. A number of critical physics issues can be identified for the CRFPR(20) design. Firstly, plasma turbulence associated with the self-generation of internal magnetic fields might increase transport. Secondly, the physics of ohmic heating to ignition (primarily depositing power in the outer plasma region) followed by alpha-particle heating (primarily central-plasma heating) has to be considered in relation to the transport and sustainment. Thirdly, equilibrium and stability considerations, including the effects of field errors, are important. Fourthly, for the compact options, it is necessary to consider steady-state reactor operation and, hence, possible current-drive schemes. Lastly, active ash/impurity control schemes based on a pumped limiter or a magnetic divertor must not adversely affect the field configuration in the outer region. Each of these five important areas are briefly addressed.

3.1.1. Transport. The transport scaling used to bracket ignition margins for the cost-optimized designs represented on Fig. 2 is in qualitative agreement with experiment[3,19] and recently published theoretical estimates for energy confinement in plasmas dominated by resistive fluid turbulence.[20,21] Although the reactor calculations have not yet taken into account effects of field errors on transport, which are important in experiment, field-ripple constraints, nevertheless, have been imposed on the TFC design.[14] The streaming parameter is monitored during the startup simulation and, through a fueling algorithm coupled to the plasma/circuit response, is not allowed to exceed a few percent at any time during the critical startup phase. The startup trajectory requires the plasma parameters to remain close to the region of minimum energy[4,5] in order to minimize transport losses and flux consumption. The key question in this area is the maintenance of the observed favorable confinement scaling with current at constant beta for reactor-like currents, current densities, and temperatures.

3.1.2. Heating. Ohmic dissipation in an RFP provides a powerful heating mechanism and yields a transport scaling of the form given in Fig. 2. Ohmic ignition with ν as low as 0.8 appears to be acceptable from the viewpoint of flux consumption. The physics scaling early in the setting-up phase may be different than that assumed, although the application of a varying scaling is not warranted by present understanding. A similar comment can be made for the conditions prevailing after startup, when the plasma heating is dominated by alpha particles $[P_\alpha/(P_\alpha + P_\Omega) \simeq 0.96]$. Ignition at values of ν below ~ 0.8 is possible only for plasmas of higher current density, further increased power density, reduced size, and higher resistive volt-second consumption. Ignition occurs for $\beta_\theta \simeq 0.05$, which is equal to or below experimentally achieved values, with subsequent alpha-particle heating and fueling control driving β_θ up to ~ 0.2 design target.

3.1.3. Stability and Equilibrium. Since the CRFPR(20) plasma contains 120 MJ (1.1 MJ/m^2 of first-wall area) of kinetic energy, current terminations must be controlled. Current terminations observed in RFPs, however, are physically different from major disruption in tokamaks, in that the large positive voltage spike observed in tokamaks is not observed and the current termination appears to be delayed in time by density and refueling control. The CRFPR(20) design assumes some form of active long-term control of plasma position by the EFCs, but the influence of a system for active feedback of local modes on the reactor design remains to be assessed. The presence of the electrically thick conducting shell required for short-term stabilization of global modes, introduces several, which may be important and generally unresolved problems. A thick shell has a strong influence on the tritium breeding as well as the impurity control scheme (i.e., limiter slots, divertor channels, non-axisymmetric perturbations), the maintenance/assembly scheme (i.e., gaps and breaks), and overall first-wall/blanket operation (i.e., thickness of conducting liquid-metal blankets, coolant flow surges, current paths in structures, etc.). Lastly, a number of unresolved questions arise when a strongly ohmically heated plasma ignites and then makes a transition to a significantly different heating profile as alpha-particle heating dominates. Alpha-particle-driven plasma oscillations can induce transport (of both fuel and ash), plasma instability and beta limits (the alpha-particle pressure at steady state increases the poloidal beta from 0.20 to 0.23), and perhaps might even affect the RFP dynamo.

3.1.4. Current Drive. The existence of a powerful and robust RFP dynamo creates the possibility for efficient current drive by oscillating the PFC and TFC circuits at low frequency ($\lesssim$ 50 Hz) and amplitude ($\lesssim$ 1%). This current-drive mechanism was first suggested by Bevir and Gray[22] and subsequently examined by others.[23] The principle of oscillating-field current drive expressed in terms of electrical elements is as follows: If the plasma behaves as a variable inductance, a DC toroidal current can be induced by applying AC voltages to the two circuits in the correct phase. This method depends on the close coupling between the poloidal and toroidal currents in the plasma as a result of the relaxation process. The energy stored and oscillated in the poloidal and toroidal current-drive circuits is estimated to be 44.5 MJ for the CRFPR(20) reactor case (50 Hz, plasma current change of $\delta I_\phi/I_\phi = 0.01$, and a toroidal flux change of $\delta\phi/\phi_0 = 0.035$). The transfer of this energy can give rise to sizable reactive power flows between the plasma and driver coils. The magnitude of this reactive power depends on the plasma magnetic-field, current, and temperature profiles, but only the fraction of this reactive power ($\delta I_\phi/I_\phi = 0.01$) actually would be handled by the current-drive power supply. The degree to which the actual current-drive circuit can be designed to provide isolation and efficient management of large reactive powers remains as a key issue.

3.1.5. Ash/Impurity Control. Both (poloidal) pumped limiters,[14] and (toroidal) magnetic divertors[24] are being considered for impurity/ash control for the compact RFP reactor. Because of the dominance of poloidal rather than toroidal fields in the RFP edge-plasma region, the geometry for each ash/impurity control scheme is generally orthogonal to that usually considered for tokamaks.

The base-case CRFPR(20) design[14,15] adopted pumped-limiter impurity control. The higher average first-wall power density expected for the compact reactor requires a greater fraction of the first-wall area to serve a limiter function in order to maintain heat- and particle-flux limits set by thermal-mechanical considerations.[15] In fact, the total first-wall area (110 m^2, with the limiter being ~ 40% of total area) for the CRFPR is comparable to the STARFIRE limiter area (~ 60 m^2) and would operate at comparable peak power densities (4-6 MW/m^2) and particle fluxes for similar edge-plasma conditions (i.e., radiation fractions, temperatures, densities, etc.). The dominant poloidal field at the scrapeoff layer favors a scheme with a toroidal array of poloidal limiters. For an array of N_L poloidal limiters, a field-line reconnection length, $L \simeq \pi r_p/N_L q$ (compared to $\pi R_T q$ for a tokamak toroidal limiter) that is sufficiently long is required for adequate radial diffusion into the scrapeoff region as edge-plasma particles follow high-pitch field lines between intersecting limiter surfaces. As for other pumped-limiter configurations, a large fraction of the plasma energy loss must be shed as radiation ($f_{RAD} \gtrsim 0.9$) in order to reduce the energy/particle load on the limiter surface. Limiter sputtering has been estimated, but uncertainties in neutral-atom transport, edge-plasma conditions, and redeposition profiles render these erosion estimates uncertain. Large gross sputtering rates are predicted, as for other fusion concepts, unless the edge-plasma temperature are very low or very high and/or larger radiation fractions (i.e., radiating plasma mantles) can be sustained. If the sputter erosion rates cannot be reduced by enhanced radiative loss, operation of efficient magnetic divertors with high edge-plasma temperatures may be necessary; in this connection, the RFP magnetic topology presents certain advantages.[24]

Toroidal-field poloidally symmetric and toroidal-field bundle divertors have been considered for the CRFPR(20) design.[24] The bundle divertor appears preferable to the symmetric divertor from a viewpoint of engineering access. The bundle divertor system, however, has currents flowing parallel to the PFC currents, resulting in larger coil forces and stored energy. The poloidally symmetric toroidal-field divertor destroys toroidal symmetry, whereas the bundle divertor destroys both toroidal and poloidal symmetry, possibly having a greater effect on plasma stability and transport. The potential to remove all or part of the bundle divertor assembly for maintenance without displacing other subsystems is an important advantage. The introduction of toroidal asymmetries by either the poloidally symmetric divertor or the bundle divertor, however, presents a physics concern, which also exists for the design with 24 poloidal limiters. Recent edge-plasma calculations,[24] using a three-dimensional field-line tracing model that includes the effects of plasma current, indicate long connection lengths (≳ 300 m), even for 24 bundle divertors; appreciable cross-field diffusion to the first-wall is expected. Since poloidally symmetric toroidal-field divertors are expected to have an efficiency of ≥ 96% along with a negligible economic impact,[15,24] this latter approach is presently under study for the RFP.[25]

3.1.6. Fueling. The requirements of the fueling scheme depends on the method adapted for ash/impurity control. Fueling by edge-plasma gas puffing is compatible only with a pumped limiter, but it should also help to protect surfaces of components within the vacuum region by maintaining a cold and dense edge plasma. To some degree divertors will require at least low-velocity pellet fueling in order to introduce fuel inside the separatrix. As for most fusion reactor concepts, deep-penetration pellets with a mass that is a small fraction of the total plasma inventory will require advanced accelerators for the production of pellets with velocities > 50-100 km/s (e.g., propulsion by rail guns or laser ablation); alpha-particle/pellet interactions may also place even greater demands on the pellet injector.[10] If gas ingestion near the edge plasma is possible, low-penetration pellets for plasmas that use magnetic divertors for impurity control should prove feasible.

3.2. Engineering and Technology. The key engineering issues identified for the compact RFP reactor arise from the need for a) high-heat-flux first-wall and limiter (or divertor-plate) surfaces, b) high-power-density liquid-metal-cooled blankets, and c) acceptable erosion and radiation lifetimes for the materials used in the fusion power core, particularly for the in-vacuum components and for radiation-hardened copper coils. These technology considerations are briefly summarized here.

Generally, given acceptable plasma confinement, the key design and technology questions center on the need for acceptable radiation-fluence lifetimes for key FPC components, which in turn reflects as a strong cost tradeoff giving improved mass usage (i.e., operating cost), plant availability (i.e., mean-time-to-repair), reliability (i.e., mean-time-to-failure), and reduced component complexity upon which materials development will have a strong influence. Given that in-vacuum components can be designed and operated with average heat fluxes of 4-6 MW/m^2, as is also required for high-heat-flux components in the lower-power-density systems, critical uncertainties in this area reduce to the partition of radiative and energetic-particle fluxes incident upon in-vacuum component surfaces and the uniformity of this deposition. The high-heat-flux alloys (copper, molybdenum, vanadium) will also require development for use in the intense fusion-neutron fluxes, although radiation fluences no greater than those necessary for other fusion approaches will be required (~ 10-20 $MWyr/m^2$). The use of self-cooled liquid-metal blankets is preferred for these higher power-density systems, because of the increased power densities within the blanket. The blanket design parameters are generally determined by the relationships between MHD pumping needs of the coolant, desirable operating blanket pressure and temperature, and the need to hold coolant/structure interface temperatures below limits set by considerations of liquid-metal corrosion. The low field and short-flow-length geometry of the compact RFP reactor, however, reduces these problems relative to superconducting systems with lengthy coolant-flow paths that must traverse strong toroidal or axial fields. The magnet development required to produce relatively small, radiation-hardened resistive coils (water-cooled copper alloy, inorganic insulation, e.g., MgO) for use outside a blanket appears to be well advanced for accelerators, although dose and damage rates will be higher for fusion application.

The design conditions suggested in Tables I and II result from a desire to maintain a minimum-cost system that would operate within realistic engineering constraints and simultaneously would assure a fusion power core that could be pretested, installed, and repaired as a single unit while representing a negligible part of the plant total direct cost. As shown by the sensitivity studies summarized in Sec. 2.1. and Ref. [15], considerable latitude exists within which key constraints can be relaxed without seriously compromising either cost or other advantages of the compact fusion reactor option. Many of the design and technology problems associated with the compact RFP reactor are materials related, and a majority of these issues appear to be common to most magnetic fusion reactors. A shift in technology development will be needed, however, to accommodate the compact approaches, with the emphasis moving away from stainless steel in-vacuum components and towards high-heat-flux alloys, away from solid tritium breeders and towards liquid-metal breeder/coolants, and away from well-shielded superconducting coils and towards radiation-hardened water-cooled copper (or possibly aluminum) coils.

4. FUTURE DIRECTIONS

The CRFPR design is presently being reassessed and subjected to a more detailed engineering study called TITAN/RFP.[25] The focus of this study is a divertor-based, high-neutron-wall-loading ($\gtrsim$ 10 MW/m^2) design that also invokes oscillating-field current drive for steady-state operation. The resistive EFC power consumption for the CRFPR(20) design amounts to 53.5 MW, which along with a desire for a more open geometry points towards cost and operational incentives for otherwise more expensive superconducting EFCs, particularly if resistive-coil divertors and more conservative physics (lower beta, flatter profiles) are assumed. The OHC and TFC, however, would remain as resistive coil system in order to retain a compact reactor torus, with the OHC being used and sized for startup conditions only; both OHC and TFC would also serve current-drive functions. Figure 5 shows cost, neutron-wall-loading, mass-power-density, startup power, and other tradeoffs for the case where the OHC is sized for full grid power applied in back-biased condition and 20% of grid power available for resistive OHC losses in forward-bias condition prior to application of current-drive achievement of steady-state operation. Somewhat higher plasma currents are required compared to the CRFPR(20) design because the peak poloidal beta has been decreased from β_θ = 0.2 to 0.13 and flatter density and temperature profiles have been assumed as suggested by recent one-dimensional plasma simulations. Generally, the higher cost associated with the superconducting EFC set and the lower mass power density

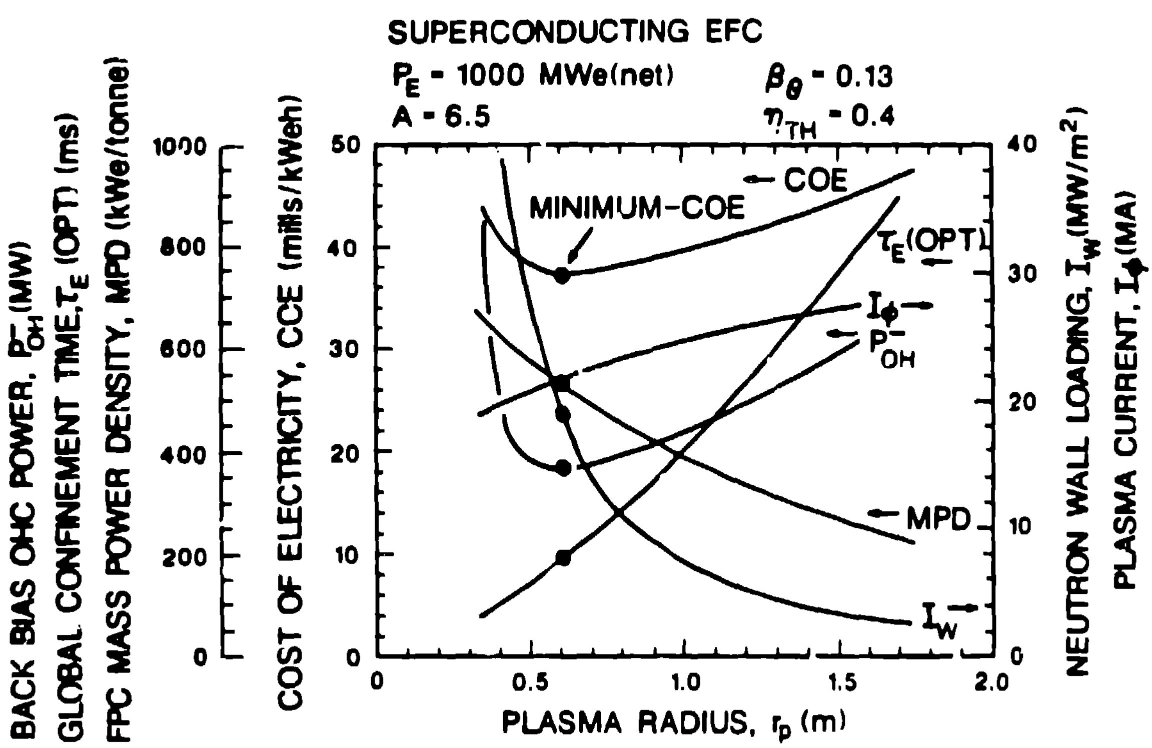

Fig. 5. Cost optimization of a divertor-based RFP reactor using superconducting EFCs, but a compact, resistive-coil (TFC, OHC) reactor torus. Shown as a function of plasma minor radius as the plasma current, I_ϕ, back-bias (grid-supplied) OHC power, P_{OHC}^-, neutron first-wall loading, I_w. optimized cost of electricity, COE (constant 1986 dollars), and FPC mass power density, MPD.

(~ 500 kWe/tonne compared to ~ 900 kWe/tonne for the CRFPR) is compensated by the lower recirculating power fractions (0.20 versus 0.18).

5. CONCLUSIONS

Ohmically heated RFP reactors have been considered with a range of neutron wall loading values, which includes conventional superconducting designs operating with low power density and compact designs with normal copper-coils and high power density. Recent emphasis has been placed on the compact approach because of substantial economic, operational, and developmental advantages. This approach is particularly suitable for high-β, poloidal-field-dominated systems where βB^2 at the plasma is large and the fields at the coils can be small; both the RFP as well as the spheromak and field-reversed configurations fall into this class. The fusion power core for this class of systems can be made comparable in mass and volume to the corresponding assembly in a fission power plant. These improved fusion reactors have a power density in the range 5-15 MWt/m^3, and a mass power density in the range 500-1000 kWe/tonne; improvements by factors of 10-30 compared with conventional designs result. Because the FPC is a smaller proportion of the total plant cost (typically 3-5% compared with 25-30%), the unit direct cost ($/kWe) is less dependent on the related physics and technology uncertainties; installation and maintenance requirements are also eased. A faster, less costly development path is also a possibility. Technological problems remain to be solved for these higher-power-density systems, however, particularly regarding high-heat-flux materials. Key physics requirements and uncertainties for the reactor include heating, transport, plasma-wall interactions, current-drive, impurity control with pumped limiters or magnetic divertors; technological considerations for each were briefly discussed. As both theoretical and applied understanding of the essential features of the RFP startup, equilibrium, impurity control, and current drive is developed, the framework design presented in Refs. 14-16 and summarized here is evolving towards a compromise between reduced technology needs and economic power density. Most recent design activities[25] remain focused on compact systems using resistive TFCs and OHCs, but with superconducting EFCs, poloidally-symmetric toroidal-field divertors, and oscillating-field current drive using carefully trimmed main-coil drivers.

REFERENCES

[1] BODIN, H. A. B. and NEWTON, A. A., "Review Paper: Reversed-Field Pinch Research," Nucl. Fus. 20, 1255-1324 (1980).

[2] BAKER, D. A. and QUINN, W. E., "The Reversed-Field Pinch," Fusion 1(A), 438 (E. Teller, ed.) (1981).

[3] BODIN, H. A. B., KRAKOWSKI, R. A., and ORTOLANI, S., "The Reversed-Field Pinch Research," submitted to Fus. Technol. (1986).

[4] TAYLOR, J. B., "Relaxation of Toroidal Plasma and Generation of Reversed Magnetic Fields," Phys. Rev. Lett. 33, 1139-1141 (1974).

[5] TAYLOR, J. B., "Relaxation of Toroidal Discharges," Proc. 3rd Topical Conf. on Pulsed High-Beta Plasmas, 59, Pergamon Press, London (1976).

[6] HANCOX, R., KRAKOWSKI, R. A., and SPEARS, W. R., "The Reversed-Field Pinch Reactor," Nucl. Eng. and Design 63(2), 251 (1981).

[7] BAKER, C. C. (Principal Investigator), et al., "STARFIRE - A Commercial Tokamak Fusion Power Plant Study," Argonne National Laboratory report ANL/FPP-80-1 (September 1980).

[8] MILLER, R. L., BATHKE, C. G., KRAKOWSKI, R. A., HECK, F. M., GREEN, L., KARBOWSKI, J. S., MURPHY, J. H., TUPPER, R. B., DELUCA, R. A., MOAZED, A., and TERRY, R. A., "The Modular Stellarator Reactor: A Fusion Power Plant," Los Alamos National Laboratory report LA-9737-MS (July 1983).

[9] BADGER, B., et al., "UWTOR-M: A Conceptual Modular Stellarator Power Reactor," University of Wisconsin report UWFDM-550 (October 1982).

[10] LOGAN, B. G. (Principal Investigator), et al., "MARS: Mirror Advanced Reactor Study," Lawrence Livermore National Laboratory report UCRL-53480 (July 1984).

[11] BATHKE, C. G., DUDZIAK, D. J., KRAKOWSKI, R. A., ARD, W. B., BOWERS, D. A., DAVIS, J. W., DEFREECE, D. A., D. E. DRIEMEYER, et al., "ELMO Bumpy Torus Reactor and Power Plant Conceptual Design Study," Los Alamos National Laboratory report LA-8882-MS (August 1981).

[12] KRAKOWSKI, R. A., HAGENSON, R. L., and MILLER, R. L., "Small Fusion Reactors: Problems, Promise, and Pathways," Proc. 13th Symp. on Fusion Technol. (SOFT) 1, 45, Varese, Italy (September 24-28, 1984).

[13] KRAKOWSKI, R. A., "Fusion Concepts with Improved Prospects for Reactors," 20th Intersoc. En. Conv. Eng. Conf (IECEC), Miami Beach, FL (August 18-23, 1985).

[14] HAGENSON, R. L., KRAKOWSKI, R. A., BATHKE, C. G., MILLER, R. L., EMBRECHTS, M. J., SCHNURR, N. M., BATTAT, M. E., LABAUVE, R. J., and WILEY, J. W., "Compact Reversed-Field Pinch Reactors (CRFPR): Preliminary Engineering Considerations," Los Alamos National Laboratory report LA-10200-MS (August 1984).

[15] COPENHAVER, C., KRAKOWSKI, R. A., SCHNURR, N. M., MILLER, R. L., BATHKE, C. G., HAGENSON, R. L., et al., "Compact Reversed-Field Pinch Reactors (CRFPR): Fusion-Power-Core Integration Study," Los Alamos National Laboratory report LA-10500-MS (August 1985).

[16] KRAKOWSKI, R. A., HAGENSON, R. L., SCHNURR, N. M., COPENHAVER, C., BATHKE, C. G., and MILLER, R. L., "Compact Reversed-Field Pinch Reactors (CRFPR)," Nucl. Eng. and Design (to be published, 1986).

[17] SHEFFIELD, J., DORY, R. A., COHN, S. M., DELENE, F. G., PARSLY, L., ASHBY, D. E. T. F., and REIERSEN, W. T., "Cost Assessment of a Generic Magnetic Fusion Reactor," Oak Ridge National Laboratory report ORNL/TM-9311 (1984).

[18] SCHNURR, N. M. and KRAKOWSKI, R. A., "Thermal Analysis of Lead-Lithium Cooled Blankets for Fusion Reactors," submitted to 1986 ASME Winter Meeting, Anaheim, CA (November 30, 1986).

[19] MASSEY, R. S., WATT, R. G., WEBER, P. G., WURDEN, G. A., BAKER, D. A, BUCHENAUER, C. J., et al., "Status of the ZT-40M RFP Experimental Program," Fus. Technol. 8(2B), 1571 (1985).

[20] CONNOR, J. W. and TAYLOR, J. B., "Resistive Fluid Turbulence and Energy Confinement," Phys. Fluids 27(11), 2676 (1984).

[21] AN, Z. G., et al., "Role of Multiple Helicity Non-Linear Interaction of Tearing Modes in Dynamo and Anomalous Thermal Transport in Reversed Field Pinch," Proc. 10th Int. Conf. Plasma Physics and Controlled Nuclear Fusion Research 2, 231 (1985), IAEA, Vienna.

[22] BEVIR, M. K. and GRAY, J. W., "Relaxation, Flux Consumption and Quasi Steady State Pinches, " Proc. RFP Theory Workshop, Los Alamos, NM (April 28 - May 2, 1980).

[23] SCHOENBERG, K. F., GRIBBLE, R. F., and BAKER, D. A., "Oscillating Field Current Drive for Reversed Field Pinch Discharges," J. Appl. Phys. 56(9), 2519 (1984).

[24] BATHKE, C. G., KRAKOWSKI, R. A., and MILLER, R. L., "A Comparison Study of Toroidal Field and Bundle Divertors for a Compact Reversed-Field Pinch Reactor," Fus. Technol. 8(1), 1616 (1985).

[25] CONN, R. W. , "The Reversed-Field Pinch as a Compact Fusion Reactor: A Program in Conceptual Reactor, Design, Technology Assessment, and Development Pathway Analysis," UCLA report (July 1985).